Sex Plant Reprod (1989) 2:231–253

Sexual Plant Reproduction

Development of the pollen grain and tapetum of wheat (*Triticum aestivum*) in untreated plants and plants treated with chemical hybridizing agent RH0007

M.B. Mizelle[1], R. Sethi[2], M.E. Ashton[3], and W.A. Jensen[4]

[1] Los Positas College, 3033 Callier Canyon Road, Livermore, CA 94550, USA
[2] 3227 Almansa Court, San Jose, CA 95127, USA
[3] Department of Biology, City College of San Francisco, San Francisco, CA 94412, USA
[4] College of Biological Sciences, The Ohio State University, 484 West 12th Avenue, Columbus, OH 43210-1292, USA

Summary. A study of pollen development in wheat was made using transmission electron microscopy (TEM). Microspores contain undifferentiated plastids and mitochondria that are dividing. Vacuolation occurs, probably due to the coalescence of small vacuoles budded off the endoplasmic reticulum (ER). As the pollen grain is formed and matures, the ER becomes distended with deposits of granular storage material. Mitochondria proliferate and become filled with cristae. Similarly, plastids divide and accumulate starch. The exine wall is deposited at a rapid rate throughout development, and the precursors appear to be synthesized in the tapetum. Tapetal cells become binucleate during the meiosis stage, and Ubisch bodies form on the plasma membrane surface that faces the locule. Tapetal plastids become surrounded by an electron-translucent halo. Rough ER is associated with the halo around the plastids and with the plasma membrane. We hypothesize that the sporopollenin precursors for both the Ubisch bodies and exine pollen wall are synthesized in the tapetal plastids and are transported to the tapetal cell surface via the ER. The microspore plastids appear to be involved in activities other than precursor synthesis: plastid proliferation in young microspores, and starch synthesis later in development. Plants treated with the chemical hybridizing agent RH0007 show a pattern of development similar to that shown by untreated control plants through the meiosis stage. In the young microspore stage the exine wall is deposited irregularly and is thinner than that of control plants. In many cases the microspores are seen to have wavy contours. With the onset of vacuolation, microspores become plasmolyzed and abort. The tapetal cells in RH0007-treated locules divide normally through the meiosis stage. Less sporopollenin is deposited in the Ubisch bodies, and the pattern is less regular than that of the control. In many cases, the tapetal cells expand into the locule. At the base of one of the locules treated with a dosage of RH0007 that causes 95% male sterility, several microspores survived and developed into pollen grains that were sterile. The conditions at the base of the locule may have reduced the osmotic stress on the microspores, allowing them to survive. Preliminary work showed that the extractable quantity of carotenoids in RH0007-treated anthers was slightly greater than in controls. We concluded that RH0007 appears to interfere with the polymerization of carotenoid precursors into the exine wall and Ubisch bodies, rather than interfering with the synthesis of the precursors.

Key words: Pollen development – *Triticum aestivum* – RH0007.

Offprint requests to: W.A. Jensen

Introduction

As part of a study of the mode of action of chemical hybridizing agents in wheat, we undertook an ultrastructural study of pollen development in *Triticum aestivum*. This paper describes the normal developmental pattern of wheat pollen and the development in plants treated with the chemical hybridizing agent RH0007.

Previous reports on pollen development in *Triticum* have compared normal and cytoplasmic male-sterile lines (de Vries and Ie 1970; Hu et al. 1977, 1979; Zhu et al. 1979; Young et al. 1979). Studies in related grasses include works on *Sor-*

ghum (Christensen et al. 1972; Christensen and Horner 1974; Warmke and Overman 1972; Overman and Warmke 1972), *Poa annua* (Rowley 1962a, b, 1963, 1964), and *Zea mays* (Skvarla and Larson 1966; Warmke and Lee 1977, 1978; Lee and Warmke 1979; Lee et al. 1979, 1980).

Materials and methods

Plants of *Triticum aestivum* L. cv 'Fielder' were grown in the greenhouse. Anther developmental stages were estimated using the stages of vegetative growth of the modified Feekes scale (Petersen 1965).

In preparation for transmission electron microscopy (TEM), spike segments bearing the middle ten florets were dissected from the plants, the lemma and palea were removed from each floret, and the anther tips were excised. The spike segments were fixed in 2% glutaraldehyde, buffered to pH 6.8 with 0.025 *M* cacodylate, for 24 h at room temperature; they were then buffer-rinsed, post-fixed for about 18 h in 1% osmium tetroxide, and dehydrated in a graded series of acetone. Individual anthers were dissected from the spike segments and embedded in Spurr's resin (Spurr 1969). Specimens were sectioned for light microscopy, stained with 0.5% methylene blue, and photographed. Specimens were sectioned for TEM, stained with 1% uranyl nitrate and Reynolds lead citrate (Reynolds 1963), and photographed on a Zeiss 109.

Male sterility was induced by RH0007, commonly called fenridazon. It is soluble in water and used with a wetting agent. Its chemical structure and toxicity follow.

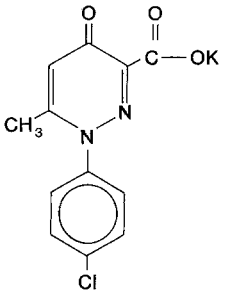

Acute primary eye irritation (rabbit)	moderate
Acute primary dermal irritation (rabbit)	slight
Acute dermal LD-50 (rabbit)	5.0 g/kg
Acute dermal LD-50 (rat)	5.0 g/kg
Fish and wildlife studies	acute and sub-acute toxicity low
Mutagenicity test	negative
Teratoloty (rat)	no teratogenicity at a dose up to 30000 ppm

No part of the treated plants was to be used for human or animal consumption.

Plants were sprayed before meiosis with 1/2 lb per acre, a dosage that causes 100% male sterility. For comparison, other plants were sprayed with 1/4 lb per acre or 1/8 lb per acre, dosages that cause 95% and 50%–75% sterility, respectively. Fixation for TEM was carried out as for controls.

Exine thickness was measured on electron micrographs for each of the stages of pollen development. Using cells from different plants and from different fixations, an average height was determined for the foot layer and the tectum minus the spines, and these quantities were summed. All measurements were made on true cross sections of the exine, where microchannels completely crossed each of the wall layers. An estimate of the total volume of wall material deposited at each stage was calculated by multiplying the wall-thickness measurement of foot and tectum times the surface area of the spherical (assumed) cells ($4\pi r^2$). Radius measurements of the microspore and pollen grain were made on light micrographs. Total cell volume was also calculated ($4/3\,\pi r^3$).

Results

Anther development was divided into seven stages: (1) precallose, (2) central callose-prophase I stage of meiosis, (3) dyad and tetrad, (4) young, free microspore, (5) vacuolate microspore, (6) vacuolate pollen grain, and (7) near-mature, 3-nucleate pollen grain. Descriptions of the developing pollen and tapetal cells will be made for each stage.

Precallose stage

The premeiotic anther of *Triticum aestivum* cv 'Fielder' consists of five cell layers: the sporogenous layer at the center, which is surrounded by one tapetal cell layer, and three outer layers that form the anther wall (Fig. 1). The sporogenous cells are the largest in the anther.

Sporogenous cells. Just prior to the onset of meiosis, the nuclear membrane of the sporogenous cells (Fig. 9) apparently blebs off many small, irregularly shaped vesicles that are prominent features in these cells (Figs. 8, 9). Their contents stain lighter than the rest of the cytoplasm. Sporogenous

Figs. 1–7. Anthers as seen in seven stages of development. **Fig. 1.** Precallose stage. Sporogenous cells at center, surrounded by one layer of tapetal cells and three cell layers of anther wall (middle layer, endothecium, and epidermis). ×448. **Fig. 2.** Central callose stage. Mass secretion of callose at center of anther forms a star-shaped figure. ×450. **Fig. 3.** Dyad and tetrad stage. The locule is formed as meiocytes separate and anther expands during meiotic division. Callose wall is thickest at cell margins. ×448. **Fig. 4.** Young, free microspore stage. Once freed from callose walls, microspores become spherical. The nucleus is spherical and centrally located in the cell, although later in this stage, it migrates to the periphery of the cell and becomes flattened. ×448. **Fig. 5.** Vacuolate microspore stage. The nucleus migrates to the inner tangential pole of the cell, the central vacuole is formed, and the cell expands. Exine-wall thickness increases. Tapetal cells begin to degenerate. ×448. **Fig. 6.** Vacuolate pollen grain stage. As mitosis and cytokinesis occur, the generative cell remains at the inner tangential pole of the cell, while the vegetative nucleus migrates toward the tapetum. Tapetal cells continue to degenerate. ×448. **Fig. 7.** Near mature, 3-nucleate pollen grain stage. As the cytoplasm proliferates, the vacuole diminishes in size and 2 sperm cells are formed (*double arrows*). The vegetative nucleus is visible (*single arrow*). Uppermost grain shows circular ER membrane figures in the vacuole that has diminished in size. ×448

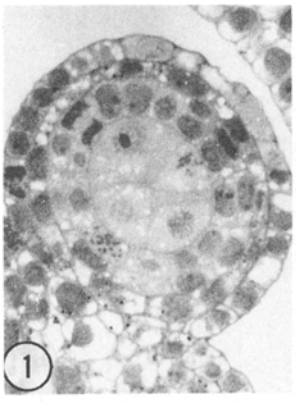
1

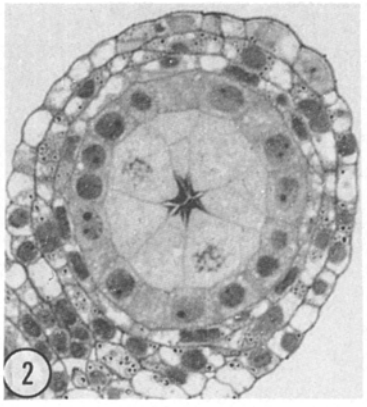
2

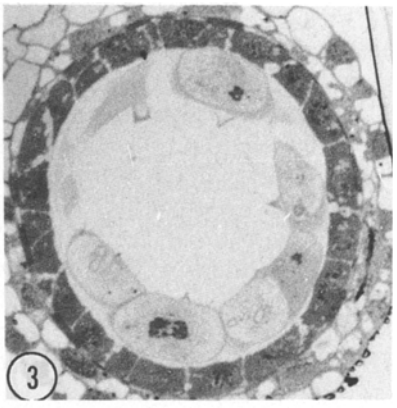
3

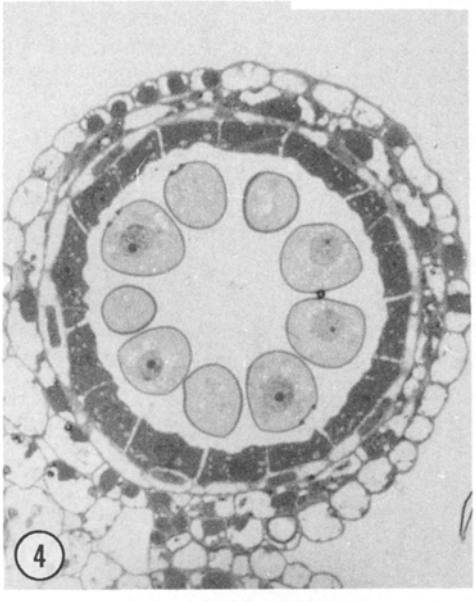
4

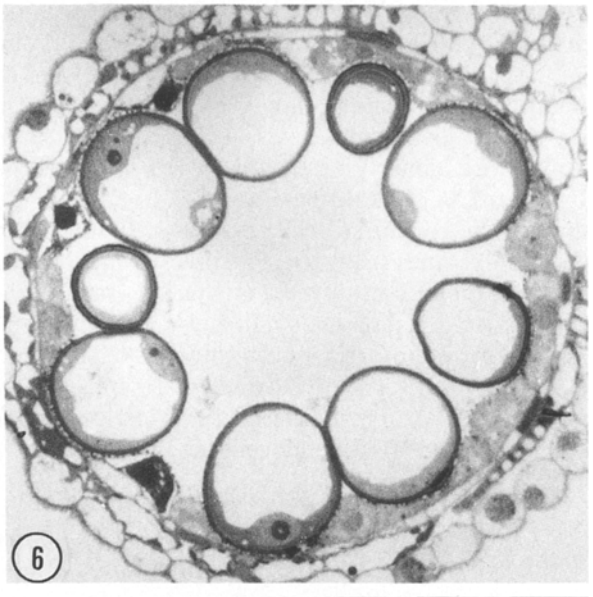
6

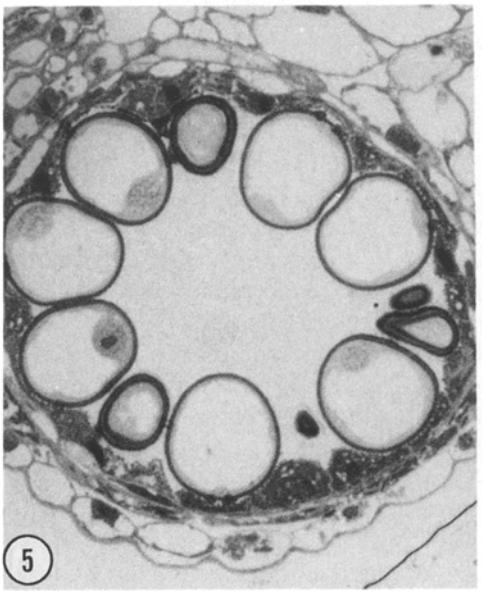
5

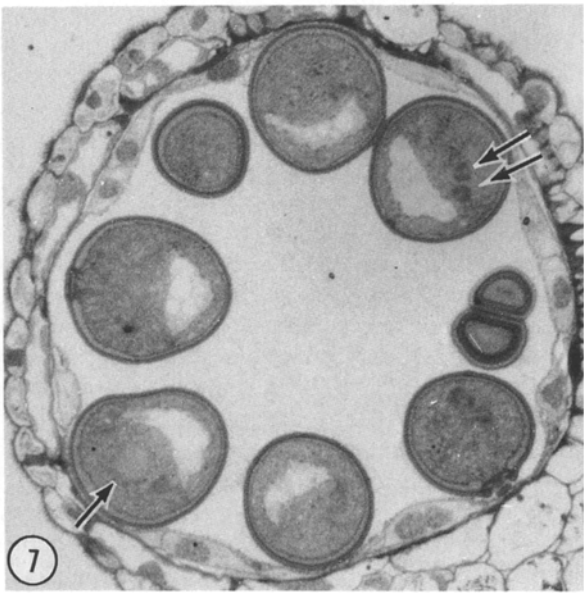
7

cell plastids vary in size and shape and stain densely. Small plastids (0.4–0.5 μm in diameter) are round or elongate, while large plastids (1.5 μm in diameter) are cup-shaped. Mitochondria are small, round, and stain lighter than plastids. A small amount of ER is present, often in circular configurations. Small vacuoles are present that contain fine granular material. Ribosomes are numerous and mostly in polysome formation. Golgi can be seen occasionally with associated vesicles (Fig. 10).

At the outer perimeter of the sporogeneous cells, protrusions from the cell wall project into the cytoplasm (Fig. 11). These are the first signs of the deposition of a callose wall that eventually will surround each sporogenous cell.

Tapetum. The tapetal cells are rectangular in outline and possess a single large nucleus (Fig. 1). Their cytosol stains more densely than that of sporogenous cells (Fig. 12). Ribosomes appear more numerous than in sporogenous cells and occur both singly and in polysomes (Fig. 13). Plastids stain densely. Mitochondria contain several cristae and stain less densely than plastids. A small network of ER is present throughout the cell. Golgi bodies are present with several associated vesicles. A number of small vacuoles are present (Fig. 12). Plasmodesmata connect adjacent tapetal cells as well as tapetal and sporogenous cells.

Central callose, prophase I stage of meiosis

Sporogenous cells. Each microsporangium has expanded in diameter, and the sporogenous and tapetal cells have enlarged (Figs. 1, 2). At the center of the anther in the sporogenous cell margins mass secretion of callose has occurred, forming a star-shaped figure in section (Fig. 2).

As meiotic prophase I begins, the sporogenous cells become separated from each other along the central callose thickenings (Figs. 14, 15). The locular space is formed here as the anther continues to enlarge (Fig. 3). Callose wall secretion continues and surrounds each sporogenous cell, isolating each of these cells inside the locule (Fig. 3).

In the nucleus, synaptinemal complexes are visible (Fig. 16). As the nuclear membrane breaks down (Fig. 18), large areas of cytoplasm that contain mostly ribosomes are seen surrounded by a double membrane that bears nuclear pores (Figs. 17, 19). The presence of the nuclear pores and the infolding of the nuclear membrane suggests that when the nuclear membrane breaks down, large segments of it remains intact and fold back on themselves to enclose areas of cytoplasm (Fig. 18). The density of the enclosed cytoplasm in larger segments appears similar to that of unenclosed cytoplasm (Fig. 17). In smaller segments, however, the interior appears more electron dense (Fig. 19), giving the impression that the contents have been condensed.

Plastids of the sporogenous cell are generally small and nearly round or elongate (Fig. 18). They contain few internal membranes. Few cup-shaped plastids were observed.

Tapetum. The tapetal cells undergo nuclear division and become binucleate during meiotic prophase I of the sporogenous cells (not shown). Condensed chromatin is commonly seen in tapetal cell nuclei (Fig. 15). The actual process of nuclear division was not observed and was assumed to take place rapidly.

The most notable feature of tapetal cells at this stage is their plastids. They are very electron dense with few internal membranes visible (Fig. 20), and they become surrounded by a narrow, electron-translucent halo. The tapetum is the only cell layer in the anther to show this phenomenon. Golgi bodies are numerous at this stage and are surrounded by many vesicles and small vacuoles with similar electron density (Fig. 21). The cytosol continues to be electron dense.

Dyad and tetrad stage

Microspores. As meiosis proceeds, the locule enlarges. Meiocytes can be seen in dyads or tetrads, each cell surrounded by a callose wall (Fig. 22). Positive identification of plastids and mitochondria is difficult, as both are light in density (Fig. 23). Occasional Golgi bodies are seen surrounded by vesicles (Fig. 23). The enclosed areas of cytoplasm seen in the last stage now contain fibrillar-granular contents, are less osmiophilic than the surrounding cytoplasm, and the surrounding membrane is fragmented (Fig. 24). Large cup-shaped plastids are few in number and are possibly in degeneration (Fig. 25), since this is the last stage in which they are observed.

Tapetum. The deposition of the tapetal orbicular wall begins at this stage. On the cell margin facing the locule, the formerly compact primary wall is seen as an expanded area of loose, fibrillar material (Fig. 26). Pro-Ubisch bodies can be seen in the cytoplasm associated with the ER (Fig. 27) and on the plasma membrane surface facing the locule (Fig. 26). Deposition of this wall has been de-

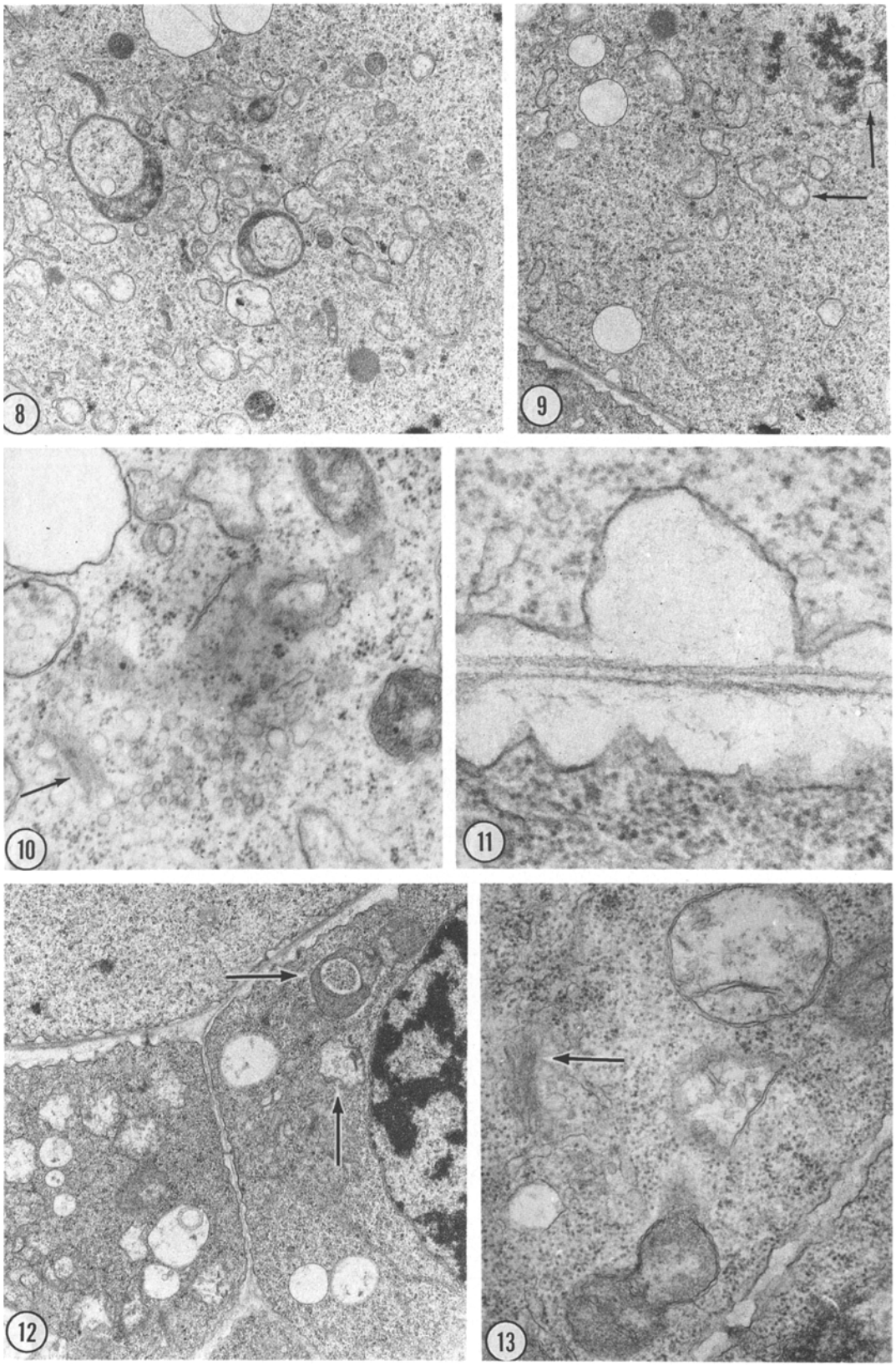

Figs. 8–13. Precallose stage. Sporogenous cells (**Figs. 8–11**) and tapetal cytoplasm (**Figs. 12, 13**). **Fig. 8.** Sporogenous cells contain large cup-shaped plastids as well as smaller ones. Two concentric ER membranes are seen on the right. ×9750. **Fig. 9.** The sporogenous cell nucleus at the *upper right* appears to bleb off irregularly shaped membrane-surrounded areas (*arrows*), also seen in Fig. 8. ×9750. **Fig. 10.** Golgi body (*arrow*) and associated vesicles in sporogenous cell. ×60000. **Fig. 11.** Protrusion of the cell wall into sporogenous cell (upper half, tapetal cell below). This is the first sign of the secretion of the callose wall that will ultimately surround each sporogenous cell. ×36000. **Fig. 12.** Tapetal cytoplasm (lower two-thirds) stains densely in contrast with microspore cytoplasm (*upper left*). Plastids stain densely (*horizontal arrow*) and mitochondria less densely (*vertical arrow*). Plasmodesmate connect two tapetal cells and tapetal cell to microspore. ×9750. **Fig. 13.** Tapetal cell with Golgi body (*arrow*) and several associated vesicles, mitochondria (*upper right*) and plastid (*lower left*). ×60000

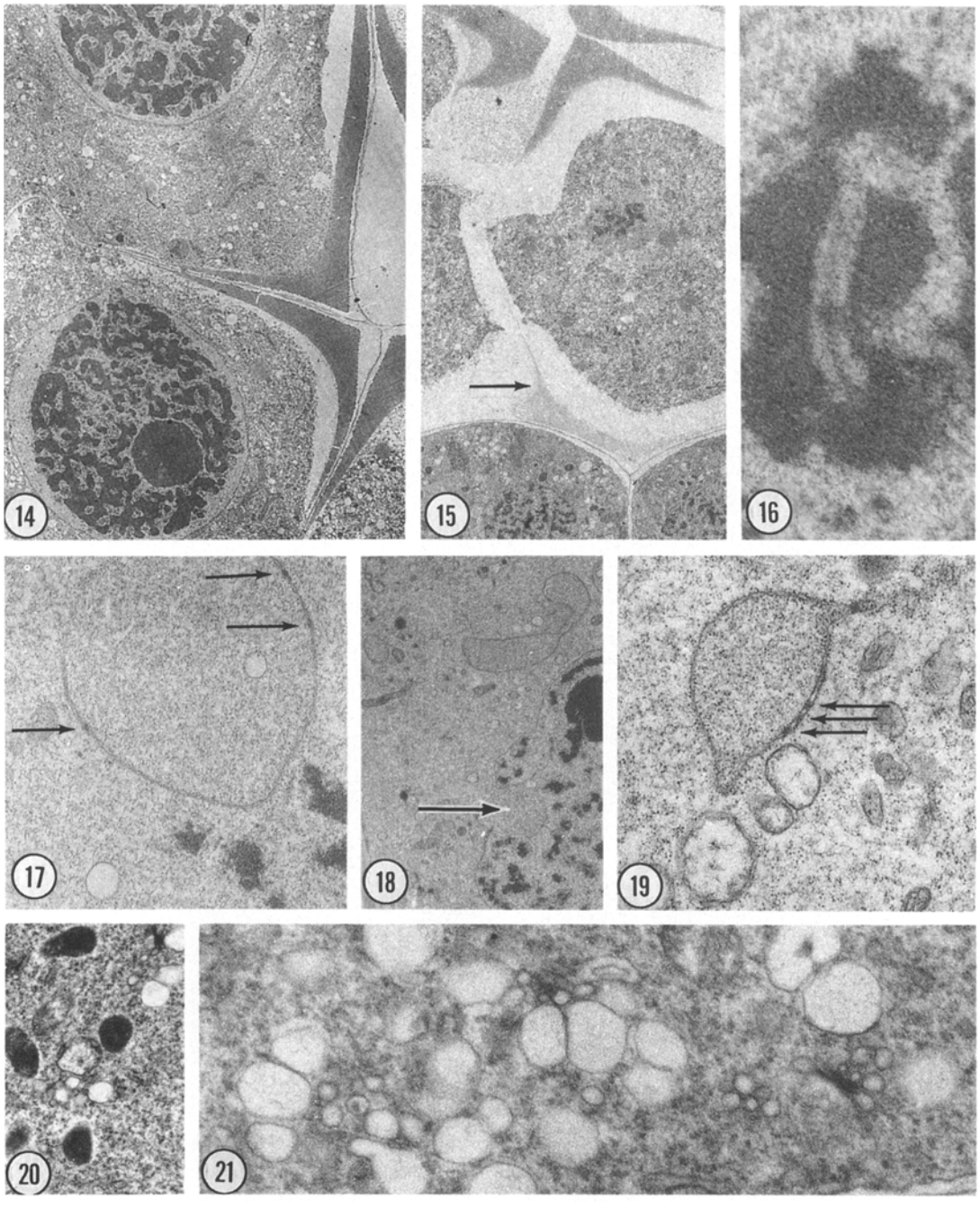

Figs. 14–21. Central callose stage. Cytoplasm of sporogenous cells (**Figs. 14–19**) and tapetal cells (**Figs. 20, 21**). **Fig. 14.** Locule formation begins as sporogenous cells separate along the margins of the central callose thickenings. × 3300. **Fig. 15.** Sporogenous cells in prophase I are completely surrounded by non-uniformly thick callose wall (*arrow*). (Sporogenous cells are plasmolyzed in this locule.) × 2250. **Fig. 16.** Synaptinemal complex of sporogenous cell of Fig. 15, seen in zygotene. × 52 500. **Fig. 17.** Membrane-surrounded area of cytoplasm. Membrane bears nuclear pores (*arrows*). Nuclear material is free in cytoplasm at *lower right*, after break-up of nucleus. × 9750. **Fig. 18.** Infolding of nuclear membrane (*arrow*), illustrating how a pocket might fuse to form a membrane-surrounded area of cytoplasm. × 3150. **Fig. 19.** A smaller membrane-surrounded cytoplasmic area with increased electron density. Nuclear pores are evident (*arrows*). × 19 500. **Fig. 20.** Halo-surrounded electron-dense plastids of tapetal cells. × 9750. **Fig. 21.** Golgi bodies of tapetal cells, surrounded by vesicles and small vacuoles. × 19 500

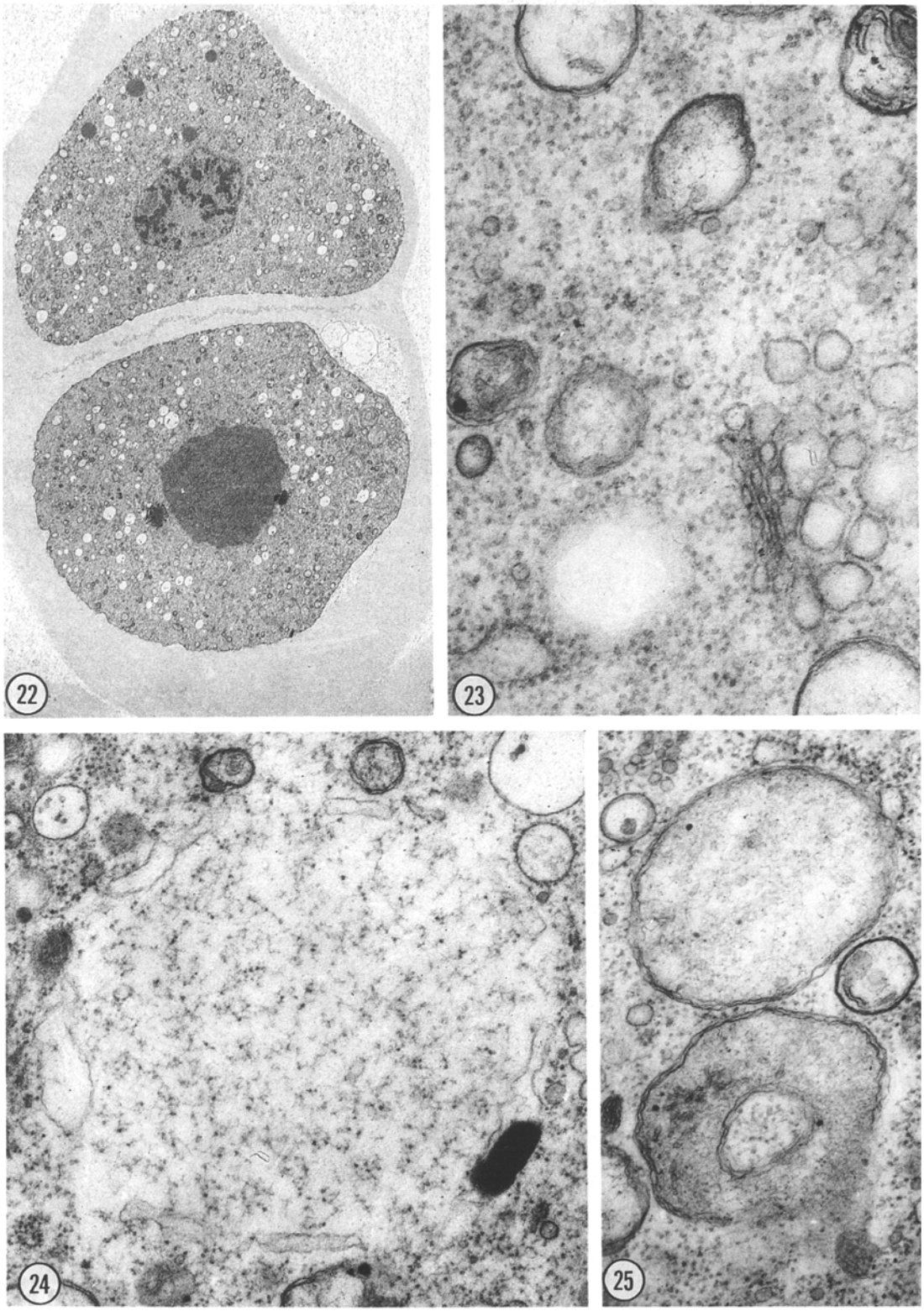

Figs. 22–25. Dyad-tetrad stage meiocytes. **Fig. 22.** Two meiocytes surrounded by callose wall. ×3300. **Fig. 23.** Golgi body and surrounding vesicles in meiocyte cytoplasm. ×60000. **Fig. 24.** Fragments of membrane-surrounded areas, which contain fibrillar-granular contents after apparent autophagic activity. ×36000. **Fig. 25.** Large plastids possibly in dissolution. They are absent from the next stage. ×22600

scribed earlier in another paper in this series (El-Ghazaly and Jensen 1986).

Tapetal plastids at this stage continue to be electron dense and surrounded by the halo. In many cases, rough ER surrounds the plastids (Fig. 28) and lies adjacent to the halo and/or to the outer membrane of the plastids (Fig. 29a, b). The outer membrane of the plastids often appears indistinct.

Young, free microspore stage

Microspores. As the callose wall disappears, each microspore becomes spherical as it separates from the tetrad (Figs. 4, 30). Early in this stage the nucleus is spherical and centrally located in the cell, but as development progresses toward vacuolation of the next stage, the nucleus migrates to the periphery of the cell and becomes flattened (referred to as offset, Fig. 31). Microspores expand throughout this stage, and by the time the nucleus has migrated, they have nearly doubled in volume (Table 1). ER segments become expanded (Figs. 33, 34) and appear to be the source of the material that will form the large central vacuole of the next stage. The exine wall rapidly increases in thickness (Table 1). Its structure has been described in detail elsewhere (El-Ghazaly and Jensen 1986). A single pore is formed and is most often oriented toward the tapetum (Fig. 30).

Microspore plastids are only of the smaller size and contain a uniformly dense matrix (Fig. 30). Some small plastids appear to undergo degeneration at this stage (Fig. 32). They contain pockets of dense matrix between some lamellae, and translucent areas between others. These degenerating plastids are absent from the next stage.

Tapetum. In this stage Ubisch bodies develop osmiophilic spikes (Fig. 35) and between the Ubisch bodies the orbicular wall network begins to form (see El-Ghazaly and Jensen 1986 for details). The loose fibrillar material that formed the original primary wall is now absent, although its outline can often be observed (Fig. 30). At this time, the primary wall between adjacent tapetal cells appears to be in dissolution. This wall area becomes wider as the locule enlarges (Fig. 36). Numerous Golgi vesicles and small vacuoles are present near the cell membrane, and some vacuoles and membranes can also be seen within the widened wall area (Fig. 36).

Halo-surrounded plastids continue to be associated with rough ER (Fig. 35). The rough ER is found throughout the cell and adjacent to the tapetal plasma membrane that is in contact with the locule (Fig. 37). In some cases the ER appears confluent with this plasma membrane (Fig. 38).

In 41% of the locules examined ($n=17$), tapetal cell plastids showed dense globules in the surrounding halo (Fig. 37). In some cases deposits were seen in the ER, and in others they were observed adjacent to mitochondria. These deposits were restricted to tapetal cells, and these cells did not appear to be in a state of degeneration.

Vacuolate microspore stage

Microspores. As the large central vacuole forms (Fig. 39), the spherical microspores expands to more than four times the volume of the young, post-meiotic microspores (Table 1). Vacuolation appears to be a rapid process, a evidenced by the presence of vacuolate cells side by side with nonvacuolate ones (Fig. 31) and by the similar diameters

Table 1. Exine wall deposition pattern and microspore volumes. *Note:* Volume of wall material deposited by the vacuolate pollen grains stage was taken as 100%. Sample sizes denote numbers of different anthers from which exine wall thickness measurements were taken. Many of the anthers were from different plants

Stage of development	Diameter of microspore or pollen grain (μm)	Volume of the microspore or pollen grain (μm)	Surface area of microspore or pollen grain (μm)	Thickness of foot and tectum (μm)	Percentage of total thickness deposited	Volume of wall material (cubic μm)	Percentage of volume deposited in each stage
Young microspore (nucleus central) ($n=6$)	22	5,575	1520	0.04	5	61	0.6
Young microspore (nucleus offset) ($n=8$)	27	10,306	2290	0.44	53	1008	10.3
Vacuolate microspore ($n=14$)	36	24,429	4072	0.73	88	2972	30.3
Vacuolate pollen ($n=8$)	47	54,362	6940	0.83	100	5760	58.8
3-Nucleate pollen ($n=2$)	50	65,450	7854	0.69	–	5419	0.0

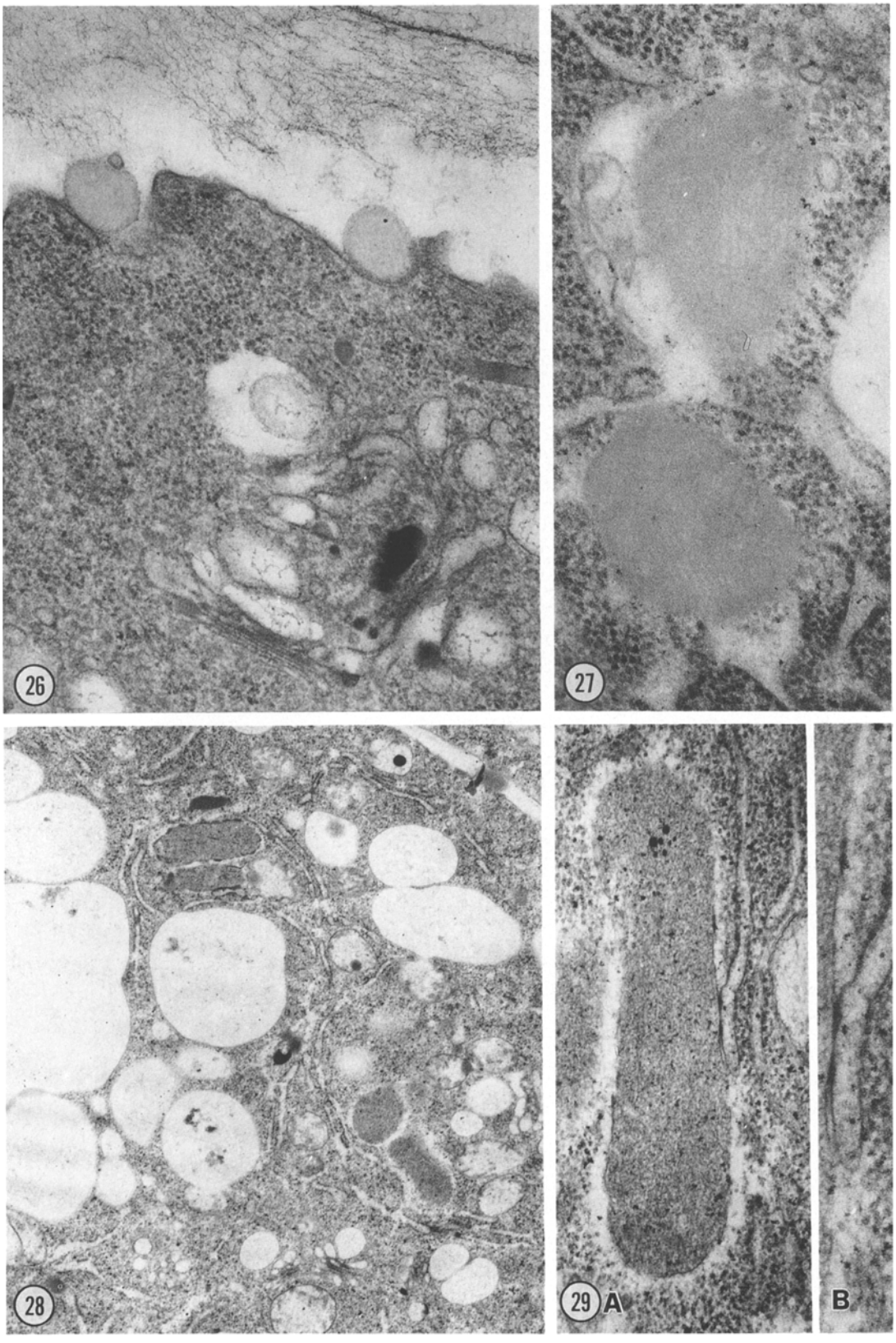

Figs. 26–29. Tapetal cytoplasm of dyad-tetrad stage. **Fig. 26.** Pro-Ubisch bodies on the tapetal cell membrane that faces the locule. The remnants of the primary wall are seen as fibrils (*above*). ×38400. **Fig. 27.** Pro-Ubisch bodies associated with the ER. ×60000. **Fig. 28.** Halo-surrounded plastids associated with ER. ×13200. **Fig. 29. A** Halo-surrounded plastid and ER membrane contiguous with the plastid outer membrane. ×60000; **B** enlarged view of ER and plasma membrane. ×84000

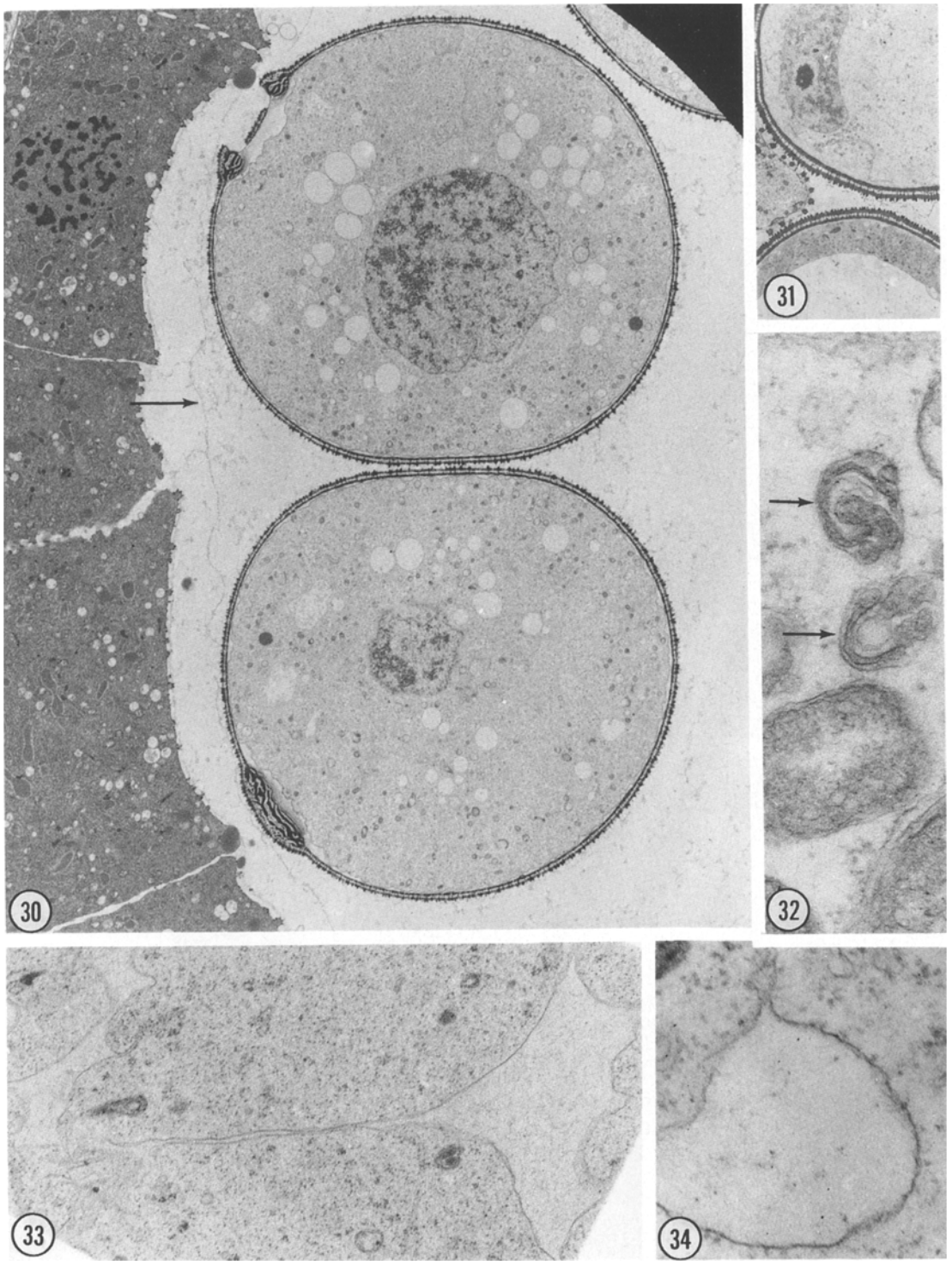

Figs. 30–34. Microspores in the young free microspore stage. **Fig. 30.** Spherical microspores, with nucleus centrally located in cell. Exine wall has a single pore. Dense tapetal cytoplasm (*left*) shows halo-surrounded plastids, pro-Ubisch bodies on cell surface and remnants of the primary wall (*arrow*). ×3000. **Fig. 31.** Nonvacuolate microspore with flattened nucleus offset in the cell (*upper cell*) adjacent to a cell that has already vacuolated (*lower cell*). ×490. **Fig. 32.** Two small plastids appearing to undergo degeneration (*arrows*). ×52500. **Figs. 33, 34.** Expanding ER segments appear to be the source of the central vacuole formed by the next stage. **Fig. 33** ×19500, **Fig. 34** ×60000

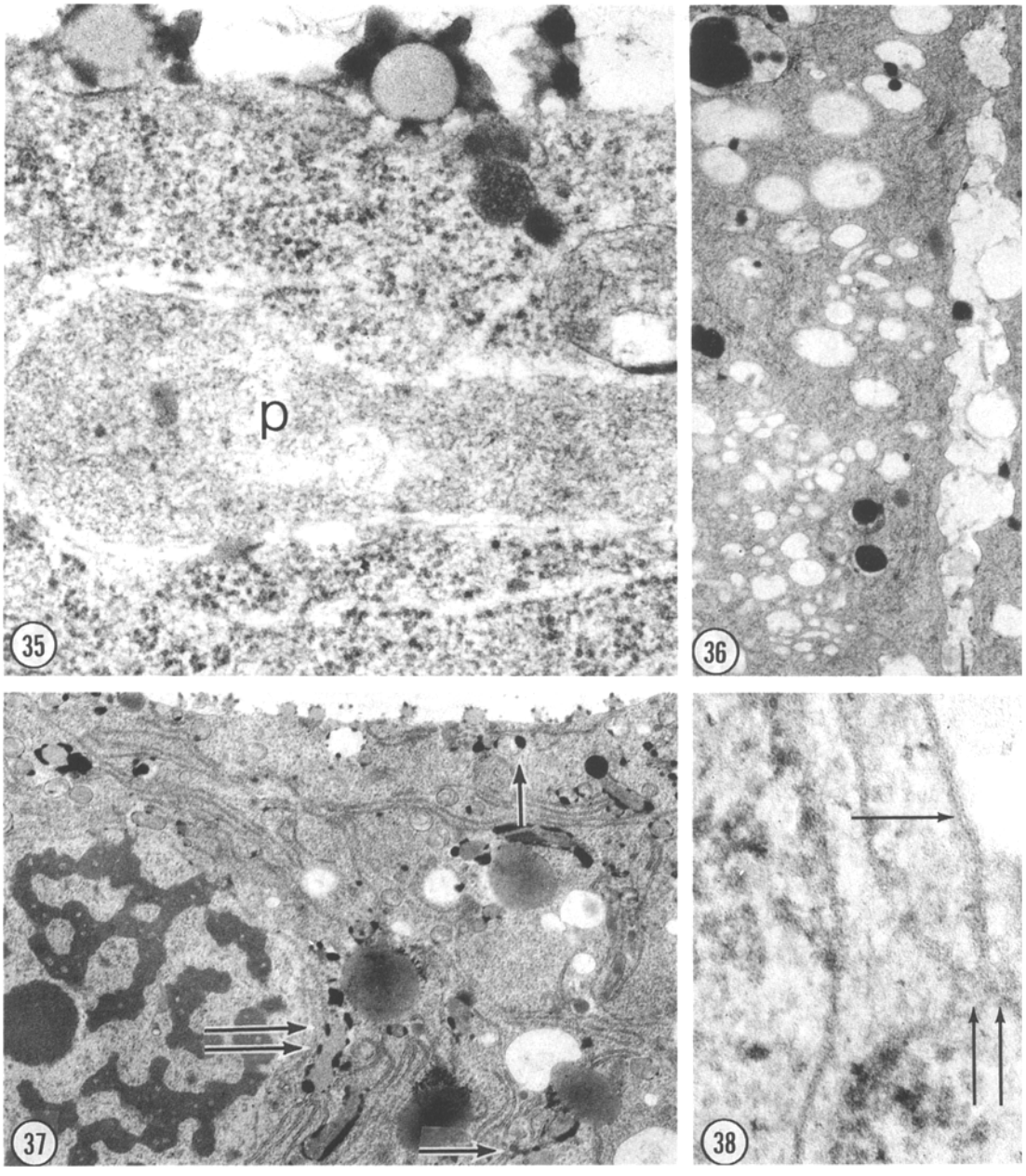

Figs. 35–38. Tapetal cytoplasm of young free microspore stage. **Fig. 35.** Halo-surrounded tapetal plastid (*p*) with ER membranes adjacent to the halo. Developing Ubisch bodies on the plasma membrane surface. × 60000. **Fig. 36.** Cell wall between adjacent tapetal cells widens and contains small vacuoles. × 9000. **Fig. 37.** Tapetal plastids with dense globules in the halo (*double horizontal arrow*), in the ER (*single horizontal arrow*), and with a mitochondrion (*single vertical arrow*). Found in 41% of the anthers examined ($n=17$). × 9000. **Fig. 38.** Tapetal plasma membrane (*single arrow*) and ER membrane appearing confluent with it (*double arrow*). × 150000

of locules containing nonvacuolate and vacuolate microspores. After vacuolation occurs, the microspore nucleus migrates to the cell pole closest to the center of the locule (Fig. 39). Exine wall deposition continues (Fig. 40), with 88% of the total cross-sectional thickness having been deposited by this stage (Table 1). The cytoplasmic organelles appear much the same as before vacuolation took place, only now they are restricted to a narrow strip of cytoplasm at the periphery of the cell. The ER proliferates and forms a single layer beneath the plasma membrane that surrounds the cell (Fig. 39).

Tapetum. The deposition of Ubisch body and orbicular wall is completed at this stage (Fig. 41). The Ubisch bodies are fully formed, and the orbicular wall now surrounds the entire tapetal cell, al-

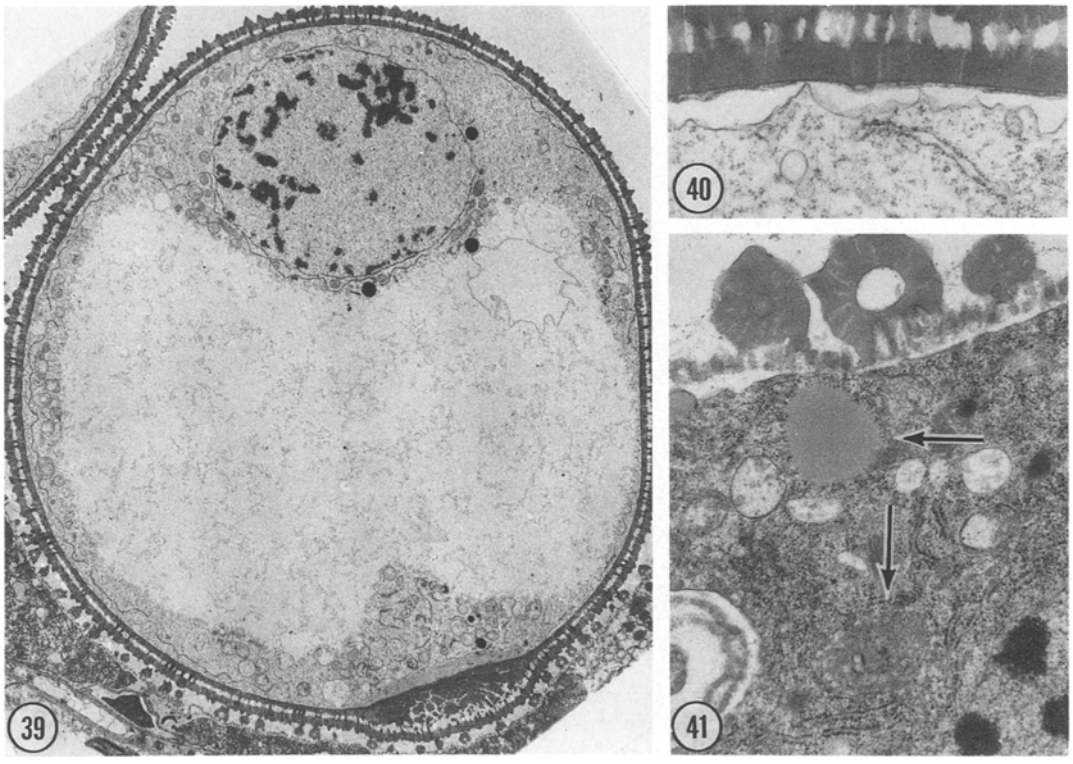

Figs. 39–41. Vacuolate microspore stage. **Fig. 39.** Vacuolated microspore with prominent nucleus and proliferating ER. ×3150. **Fig. 40.** Exine wall (*above*), and proliferating ER of vacuolated microspore cytoplasm. ×19500. **Fig. 41.** Tapetal cell with mature Ubisch bodies (*above*) and enlarged degenerating plastid (*vertical arrow*), no longer surrounded by a halo. Lipid deposit begins to accumulate (*horizontal arrow*). ×19500

though the Ubisch bodies are restricted to the surface facing the locule (see El-Ghazaly and Jensen 1986 for details). The tapetal cells appear to have been compressed by the expanding microspores (Fig. 5), and their degeneration begins at this stage. Plastids show the first signs of degeneration. They become enlarged and their previously prominent halo has disappeared (Fig. 41). Spheres of lipid deposit accumulate in the cells. Golgi body number is markedly decreased, as well as the number of small vesicles and vacuoles. The density of the cytosol decreases, and the rough ER membranes become prominent.

Vacuolate pollen grain stage

Pollen grains. At the time of mitosis the microspores have expanded to nearly ten times their original volume (Table 1). Cell division is unequal, with the large vacuole and most of the cytoplasm becoming part of the vegetative cell (Fig. 42A). After cytokinesis the vegetative nucleus migrates to lie adjacent to the tapetum (Fig. 6). The small generative cell remains near the locule center (Fig. 6) but will later detach from the wall and migrate to occupy a position within the vegetative cytoplasm. Cytoplasmic changes occur rapidly at this stage (Fig. 42A, B): the number of ribosomes increases – many of which are in polysome formation; plastids increase in number and begin to accumulate starch; mitochondria increase in number and form prominent cristae; the rough ER proliferates, expands, and accumulates dense granular material; and Golgi bodies proliferate, accompanied by vesicles. Intine wall deposition begins immediately following the mitotic division and continues throughout this stage (Fig. 42B, see El-Ghazaly and Jensen 1986 for details). Exine wall deposition also continues, with the maximum cross-sectional thickness being achieved in this stage (Fig. 42A).

Tapetum. The degeneration phase continues, and the cells become further compressed (Fig. 6). The cytosol appears precipitated (Fig. 42C). Degenerating plastids become larger and now contain many concentric membrane figures, each surrounding a granular mass (Fig. 42C, D). Spherical lipid deposits continue to accumulate in the cells

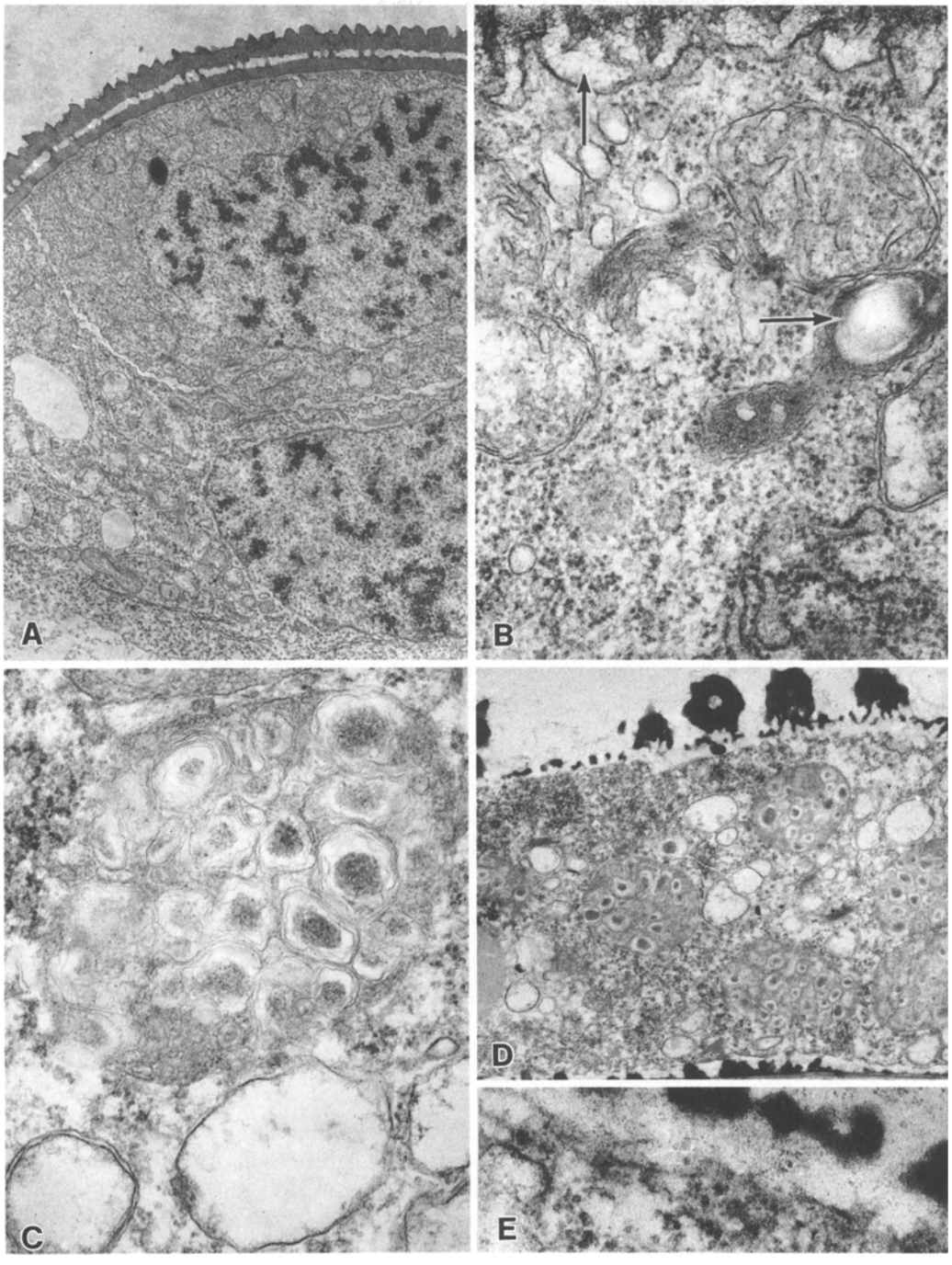

Fig. 42A–E. Vacuolate pollen grain stage. **A** Generative cell (*above*) and vegetative nucleus (*below*) of vacuolate pollen grain. ×4800; **B** pollen-grain plastids with accumulation of starch (*horizontal arrow*). Intine-wall formation begins (*vertical arrow*). ×60000; **C** enlarging tapetal plastid that contains concentric membrane figures. ×60000; **D** tapetal cytoplasm with enlarged degenerating plastids, lipid deposit (at *lower left*), and mature Ubisch bodies on orbicular wall (*above*). ×9000; **E** discontinuous tapetal plasma membrane (orbicular wall above). ×60000

(Fig. 42D). Although the plasma membrane and ER membranes become discontinuous (Fig. 42E), the cell contents remains within the orbicular wall.

Near mature, 3-nucleate pollen stage

Pollen grains. The pollen grains have enlarged to nearly 12 times the volume of the post-meiotic microspores (Table 1). The thickness of the exine wall

decreases slightly at this stage, possibly due to stretching with continued cell expansion. The intine wall continues to increase in thickness to nearly twice that of the exine (Fig. 7), with greater thicknesses near the pore area (see El-Ghazaly and Jensen 1986). The cytoplasm proliferates, nearly filling in the central vacuole (Fig. 7). Circular ER membrane figures are seen throughout the vacuole (Fig. 7).

Plastids are numerous, each being completely filled with one large starch grain (Fig. 43A). Mitochondria are numerous and contain many cristae (Fig. 43C). The network of rough ER is extensive, and cisternae are further distended with granular-fibrillar deposits (Figs. 43B, C). The cytoplasm is dense with ribosomes, most of which are in polysome formation.

The generative cell has divided into two sperm cells (Figs. 7, 43A), each of which has a long "tail" region (Fig. 43B). Like the generative cell but atypical of most cells, the sperm are completely surrounded by the cytoplasm of the vegetative cell. The sperm are easily recognizable by the adjacent undulating pair of plasma membranes of the sperm and vegetative cell (Fig. 43A, D). Mitochondria, a small amount of ER (Fig. 43F), and Golgi bodies (Fig. 43G) are present, but no plastids were observed.

Tapetum. Tapetal cells are further compressed (Fig. 7). In some locules degenerating plastids and mitochondria remain recognizable along with lipid deposits and short segments of ER (Fig. 43E).

Pattern of exine deposition

Exine thickness measurements gave a static picture of wall deposition: 38% of the wall thickness is deposited during the young microspore stage; 50% during the vacuolate microspore stage; and 12% during the vacuolate pollen grain stage. Taking into account the increase in surface area that occurs with cell expansion, the volume of wall material deposited during each stage of development was calculated (see methods). This picture revealed more accurately that 10.9% of the volume of the exine was deposited during the young microspore stage, 30.3% during the vacuolate microspore stage, and 58.8% in the vacuolate pollen grain stage (Table 1).

Treated plants

The pattern of anther development through meiosis seen in plants treated with RH0007 is similar to that of untreated plants. (Unless otherwise noted, all observations refer to plants treated with 1/2 lb per acre, the dosage causing 95% male sterility.)

Treated/young microspore stage

Microspores. In control plants microspores are spherical (Fig. 5), while in treated plants microspores have varied shapes. Very young microspores with thin exine walls have amoeboid shapes (Figs. 44B, 46A), while cells with slightly thicker walls have shapes that are closer to being spherical (Fig. 44A). The latter are often plasmolyzed. Their exine wall has three layers, as in control microspores, but sporopollenin is added unevenly and in much reduced amounts (Fig. 46B). Calculations of the volume of sporopollenin deposited by the end of the young microspore stage showed an inverse ratio to the dosage of RH0007 applied: microspores of plants treated with 1/2 lb per acre had a wall that was 30% the volume of the control microspores; plants sprayed with 1/4 lb per acre, 39%; those sprayed with 1/8 lb per acre, 55% (Fig. 45).

Tapeta. Two patterns of development were evident and were found in both treated and in control plants. Locules either contained tapetal cells with rectangular contours as described for the controls (Fig. 44A) or cells that expanded and protruded into the locular space (Fig. 44B). In control plants at this stage, 65% of the locules ($n=17$) contained tapetal cells with rectangular contours, while in treated plants only 33% ($n=12$) had rectangular contours. Degeneration in expanded tapeta occurred at a later stage than tapeta with rectangular shapes.

The deposit of sporopollenin on pro-Ubisch bodies in treated plants is sparcer (Fig. 46C) than in the controls. In the majority (69%) of the treated locules examined ($n=13$), the tapetal plastids were surrounded by a halo, as described for control plants (Fig. 46C). Dense globules (Fig. 46D) were present in the halo in 31% of locules, compared to 41% ($n=17$) in the controls. When present, the globules were also found in the ER, and in some cases with mitochondria. In some locules they also dotted the outside surface of the plasma membrane (Fig. 46C).

Treated/vacuolate microspore stage

Microspores. Some microspores abort before vacuolation takes place (Fig. 47A). They are plasmo-

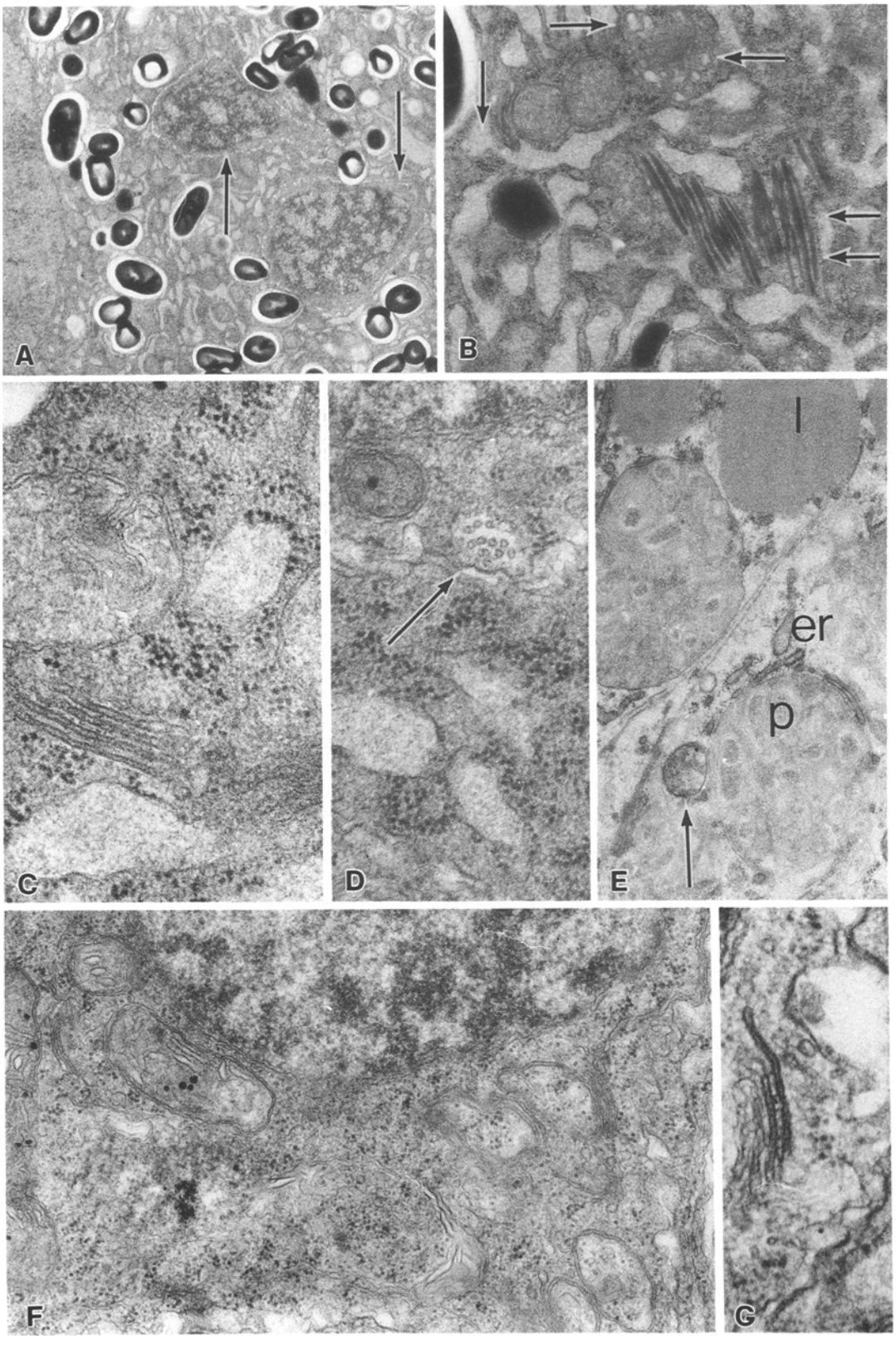

Fig. 43A–G. Near-mature, 3-nucleate pollen stage. **A** Pollen grain with two sperm (*arrows*) and vegetative nucleus at *left*. Plastids containing starch are numerous. ×4800; **B** pollen cytoplasm with extensive network of ER with distended cisternae that contain granular-fibrillar deposits (*vertical arrow*). Groups of crystalline rods (*double horizontal arrow*) are seen associated with sperm "tail". Undulating plasma membranes surround the "tail" (*two separate horizontal arrows*). ×19500; **C** mitochondria, Golgi body, polysomes and distended ER cisternae of vegetative cell. ×60000; **D** sperm cytoplasm (*upper half* of photo) containing a group of microtubules that encircle the cell (*arrow*). ×52500; **E** degenerating tapetal cell cytoplasm with mitochondrion (*arrow*), ER fragment (*er*), enlarged plastids (*p*), and lipid deposits (*l*). ×19500; **F** sperm cytoplasm containing mitochondria, ER, ribosomes, and nucleus (*above*). Undulating plasma membrane of the sperm is *below* (*left*). ×36000; **G** Golgi body of sperm cytoplasm. Undulating plasma membrane is at *upper right*. ×60000

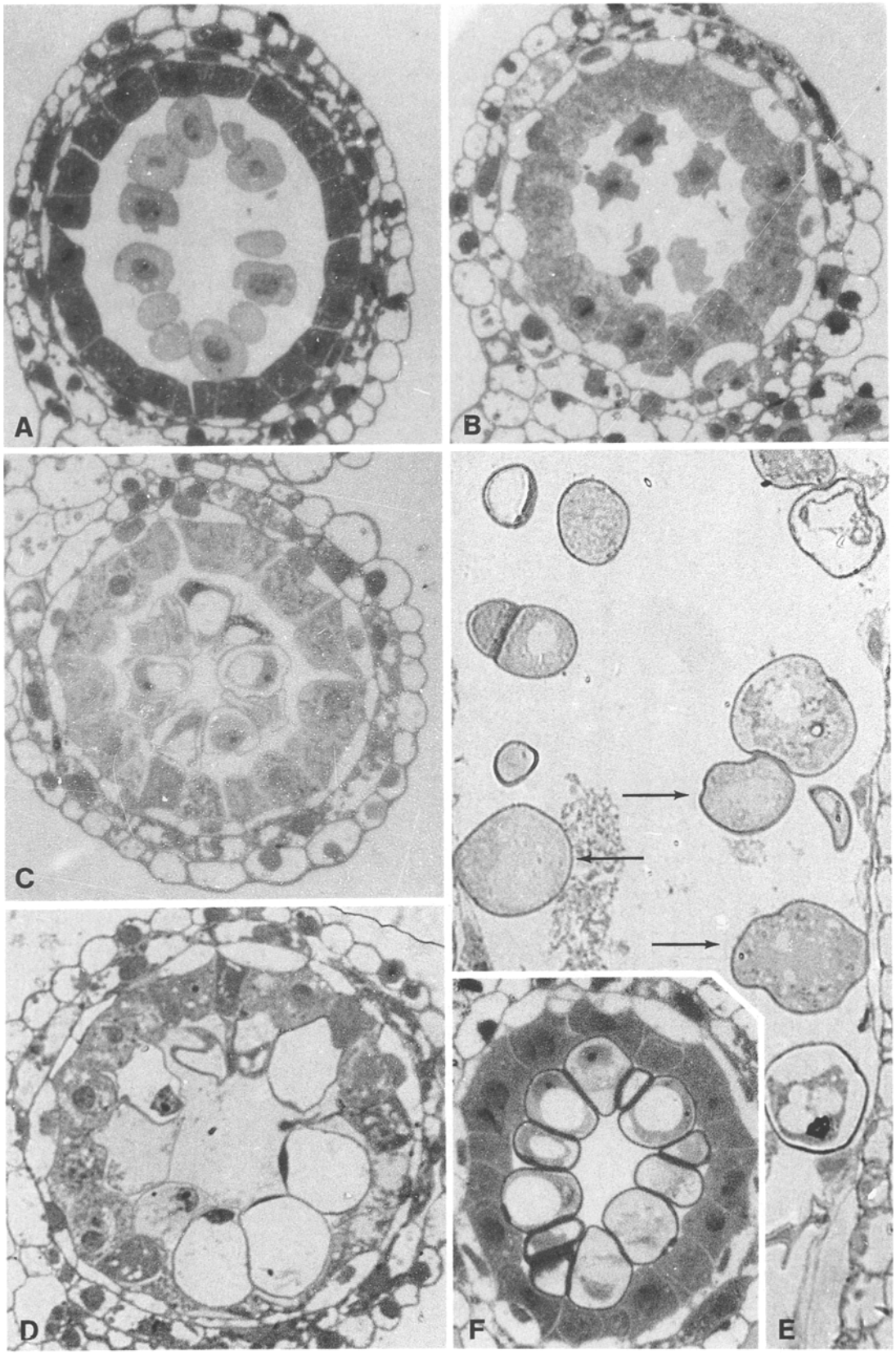

Fig. 44A–F. Anther development in plants treated with one-half, lb RH0007, (**A–E**), and control microsporangium with expanded tapetum (**F**). **A** Young microspores. Tapetal cells have rectangular shapes. ×448; **B** very young microspores with amoeboid shapes. Tapetal cells have expanded into the locule. ×448; **C** plasmolyzed microspores in the process of vacuolating. Tapetal cells are expanded. ×448; **D** vacuolated microspores with thin peripheral layer of cytoplasm. Tapetal cells are expanded and degenerating. ×448; **E** "Breakthrough" pollen grains that survived RH0007-treatment (*arrow*), but generative cell did not divide to form sperm. ×448; **F** untreated, control microsporangium with vacuolate microspore and expanded tapetal cells. ×448

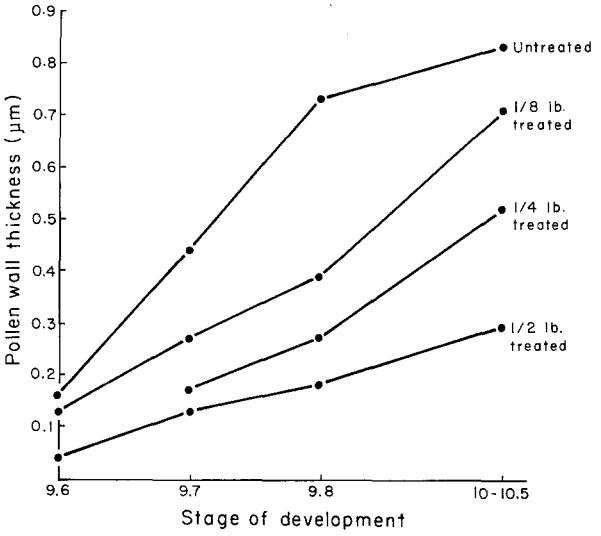

Fig. 45. Effect of concentration of RH0007 on microspore-wall thickness. Young microspore (stage 9.6), vacuole microspore (stage 9.7), vacuolate pollen grain (stage 9.8) and near-mature, 3-nucleate pollen (stage 10–10.5)

lyzed and have ruptured plasma membranes and precipitated cytosol. Degenerating plastids have a dense matrix between some lamellae and transparent between others (Fig. 47B). Dense globules are associated with these plastids (Fig. 47B). Golgi bodies become circular (Fig. 47C), and ER membranes are disrupted and clumped together (Fig. 47A). The exine wall in these cells has a wavy contour (Fig. 47E) and is 51% of the thickness of that of the controls (Fig. 45).

In other plasmolyzed microspores, vacuolation took place. Later in the stage, the degenerating cytoplasm formed a very thin, dense layer at the periphery of the cell (Fig. 47D). Small lipid droplets appeared to bleb toward the vacuole (Fig. 47D).

Tapeta. Degeneration begins with plastid enlargement (Fig. 46E), as in the controls. The plastid halo is no longer present, although the ER, now disrupted, remained associated with the plastids. As degeneration continues, membrane whorls are observable in the plastids, but they more faint than seen in controls (Fig. 46F). Near the plasma membrane some plastids appear dense and unenlarged, a pattern not found in controls (Fig. 46F, arrow). Sporopollenin deposit on the Ubisch bodies continues to be sparce. In 89% of the treated specimens at this stage ($n=10$) tapetal cells were of the expanded type.

"Breakthrough" grains

In one 1/2-lb-treated locules, several microspores at the base of the anther survived, went through the mitotic division, and the pollen grain vacuole became filled in with cytoplasm (Fig. 48). They failed to proceed through a second mitosis, however, as no sperm were found. The exine wall was 35% the thickness of that of untreated pollen grains (Fig. 45), although a large intine was present. Plastid and mitochondrial proliferation took place, but only a fraction of the starch accumulation seen in controls had taken place. ER expansion and storage occurred, but the cisternae were much wider and less densely granular than what was observed in the controls.

Discussion

Development of microspore/pollen grains

Throughout development, microspores of *Triticum* are engaged in cell expansion. Overall, they experience a near 12-fold increase in volume from the young, free microspore stage to the mature, 3-nucleate pollen grain stage, as also reported by Bennett et al. (1973). We concluded that the major activity of the young microspores is cytoplasmic proliferation, since the number of organelles per unit area of cytoplasm prior to the vacuolation stage appears similar both before and after a doubling of cell volume. Plastid and mitochondrial divisions in developing pollen grains have been documented for *Zea* (Lee and Warmke 1979).

As sporogenous cells enter meiosis, localized autophagic activity appears to be taking place. With the onset of prophase I and the dismantling of the nuclear membrane, large sheets of the nuclear envelope apparently break off. Each segment appears to fuse into a separate enclosing structure that isolates an area of cytoplasm containing mostly ribosomes. Similar structures were reported in lily pollen development (Dickinson and Heslop-Harrison 1970). Ribosome numbers were also shown to fall substantially during meiosis in lily (Dickinson and Heslop-Harrison 1970), possibly due to autophagic activity in such structures. Acid phosphatase activity was localized in similar structures in female meiocytes of *Capsella* (Schulz and Jensen 1981). It is thought that ribosome destruction is related to the passage of the sporogenous cells from the diploid phase to a new pattern of development in the haploid phase (Heslop-Harrison 1968, 1971). Remnants of these structures seen in the tetrad stage in our material suggested that autophagic activity has taken place.

Vacuolation in the microspores is a rapid process. Just prior to vacuolation provacuoles form at the tips of ER segments and apparently fuse

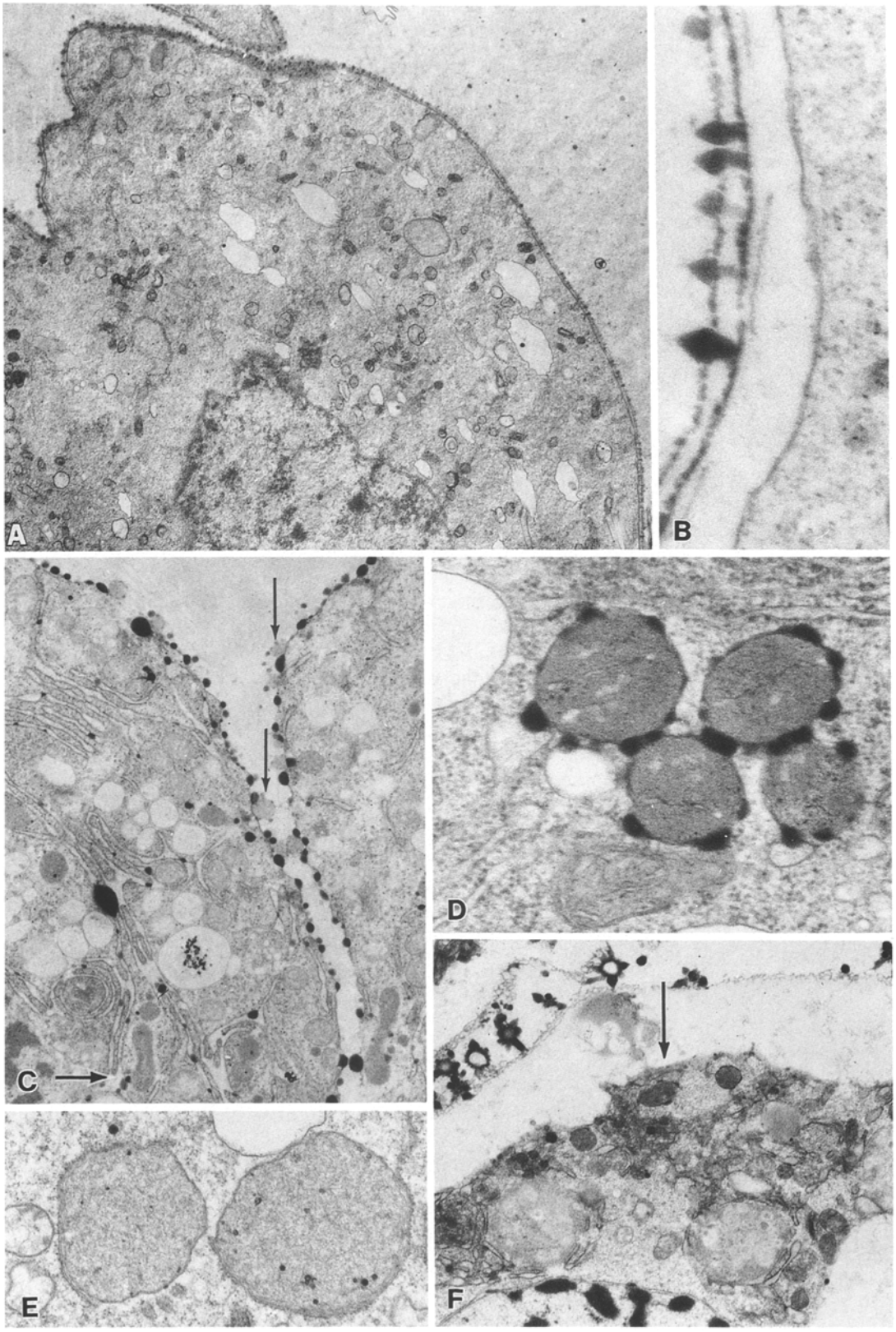

Fig. 46 A–F. Microspores of plants treated with 1/2 lb RH0007. **A–D** Young microspore stage; **E, F** vacuolate microspore stage. **A** Amoeboid-shaped microspores. ×9750; **B** microspore wall of treated plant. Deposit of sporopollenin is sparce and uneven. ×52500; **C** expanded tapetal cells of treated plant. Plastids are surrounded by a halo and associated with ER (*horizontal arrow*). Deposit of sporopollenin on pro-Ubisch bodies is sparce (*vertical arrows*). Dense globules can be seen near plastids, in ER, and on outside surface of cells. ×9000; **D** tapetal plastids with dense globules in surrounding halo, as seen in 31% of the anthers examined ($n=13$ anthers, many from different plants). ×52500; **E** tapetal plastids of early vacuolate microspore stage begin degeneration by enlarging. ×19500; **F** tapetal cell in degeneration phase late in vacuolate microspore stage. Plastids are enlarged and filled with concentric membranes. Some plastids near the plasma membrane surface (*arrow*) appear to be unenlarged and not to be degenerating. Ubisch bodies contain a small amount of sporopollenin. ×9000

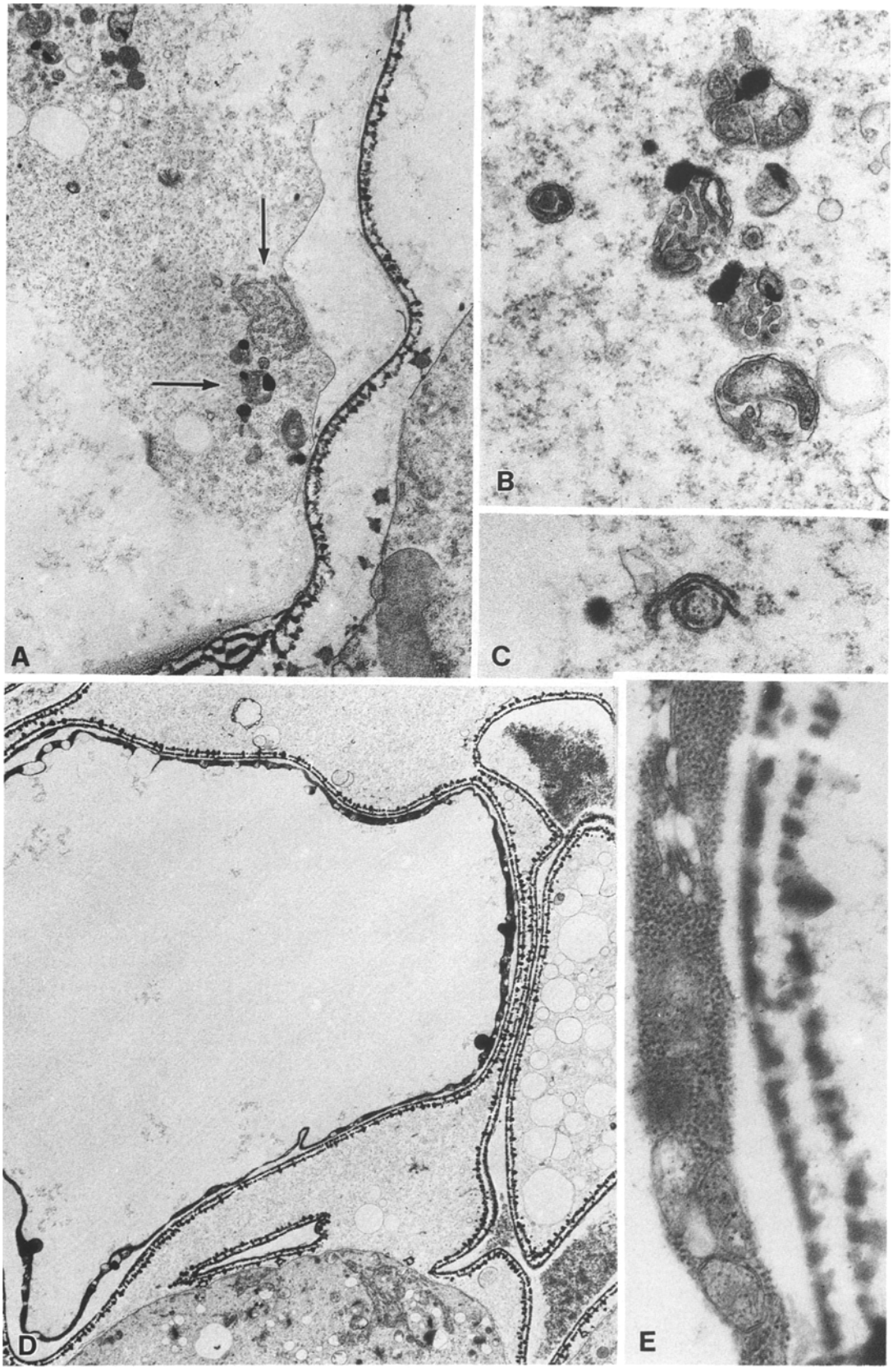

Fig. 47 A–E. Vacuolate microspore stage of plants treated with 1/2 lb RH0007. **A** Aborted microspore that did not vacuolate. Some plastids are associated with dense globules (*horizontal arrow*). ER membranes are disrupted (*vertical arrow*) ×9000; **B** degenerating plastids of aborted microspore appear similar to those of controls, except for associated dense globules. ×36000; **C** Golgi body of aborting microspore became circular. ×36000; **D** vacuolated microspore with thin, dense layer of degenerating cytoplasm. ×36000; **E** high magnification of dense microspore cytoplasm and exine. ×52500

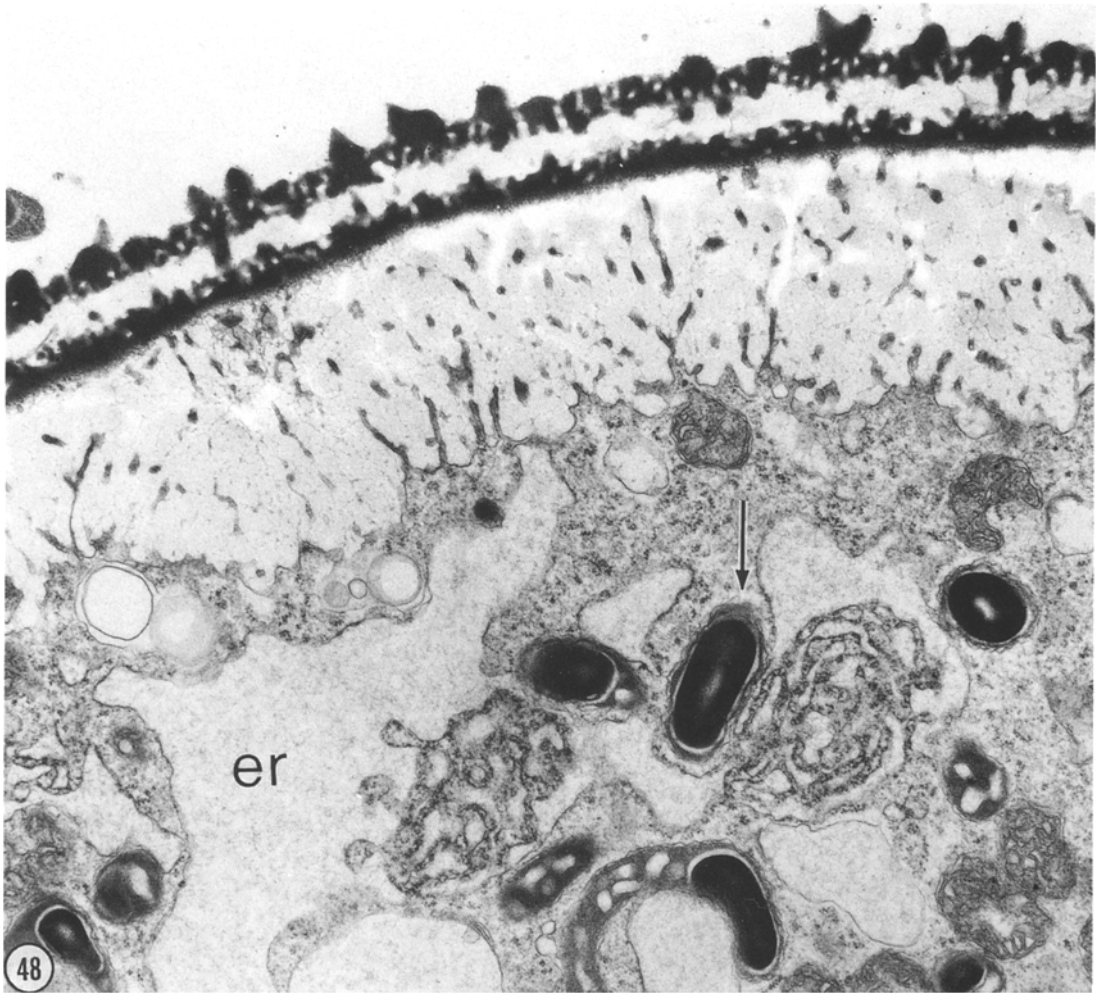

Fig. 48. "Breakthrough" sterile pollen grain found only at base of locule of RH0007-treated plant. Plastids accumulate less starch than controls (*arrow*). ER (*er*) is more expanded and with less granular deposit than found in controls. Intine wall appears normal, but exine has 51% less sporopollenin compared to controls. ×19500

to form the tonoplast membrane and the vacuolar contents. Similar provacuoles have been reported in *Triticum* by Hu et al. (1977). During the process of vacuolation, the microspores undergo more than a doubling in volume, and the exine wall thickness increases 35%, suggesting rapid deposit of wall precursors.

Once mitosis takes place and the pollen grain has been formed, the cytoplasm of the vegetative cell proliferates and begins a storage phase. Plastids increase in number, and each accumulates one large starch grain. In our material, starch accumulation always began after the first mitosis, although it was reported to have occurred in the vacuolate microspore stage in *Triticum* by Hu et al. (1979). The rough ER proliferates and its cisternae dilate and begin the storage of granular material. Golgi proliferate, and their vesicles are found near the developing intine wall, as was similarly shown for *Helleborus* (Echlin 1969). A very marked increase in polysomes occurs during this stage.

Vacuolate pollen grains are easily distinguished from vacuolate microspores by the presence of intine wall, the deposition of which begins immediately after the first mitotic division. The ER storage phase found in the vegetative cell does not occur in the generative cell or in the two sperm cells derived from it. Plastids are present in the generative cell cytoplasm, but were not found in the sperm cells and are presumed to have degenerated, as was reported by Hu et al. (1979).

The deposit of exine wall takes place rapidly during microspore/pollen grain development. During the young microspore stage, increases in the cross-sectional thickness of the wall are pro-

nounced, and the rapid increase in cell volume further demands a considerable increase in wall deposit. To described the timing of exine deposit in *Poa* pollen, which undergoes a 34-fold increase in volume in development, Rowley (1964) calculated the increase in surface area and reported the greatest increases occurred during two stages: the young microspore stage and the near-mature pollen stage. Carrying the analysis one step further in *Triticum*, we calculated the volume of sporopollenin deposited and found the majority (58.8%) of sporopollenin was deposited during the vacuolate pollen grain stage, with 10.9% deposited in the young microspore stage and 30.3% during the vacuole microspore stage. The differences in the timing of exine deposits between *Poa* and *Triticum* may in part be due to a much smaller, 12-fold increase in volume in *Triticum* pollen. During the final stage of maturation, the exine wall undergoes a decrease in thickness, as was also shown for *Poa* (Rowley 1964). Rowley speculated, as do we, that this is due to a stretching of the exine during an increase in cell volume, but with no further addition of wall material.

Tapetal developmental pattern

The tapetum in *Triticum* is of the secretory type, which is typical of grasses (Maheshwari 1950). Tapetal cells undergo mitosis, becoming binucleate during the stage of meiotic prophase I of the sporogenous cells. Development of the tapetal orbicular wall begins during the tetrad stage of meiosis and is completed before microspore vacuolation occurs (El-Ghazaly and Jensen 1986).

Senescence in tapetal cells is initiated during the vacuolate microspore stage. The first sign of senescence is the expansion of the plastids that later become filled with concentric whorls of membrane. Although the tapetal plasma membrane becomes fragmented, the degenerating cytoplasm remains within the orbicular wall and does not enter the locule. The degeneration of the tapetum has been speculated to be a process that makes extra nutrients available to the developing pollen (Maheshwari 1950), but it is also important for the occurrence of normal dehiscence of the anther.

The tapetal plastids undergo the most unusual of all the changes found during anther development. In the precallose and central callose stages, the plastid matrix is darker than the cytosol, and each plastid contains several lamellae. At the beginning of the meiosis stage, these organelles become surrounded by an electron-translucent halo, and the plastid matrix becomes very electron dense, with few lamellae visible. In the next stage, rough ER is often seen adjacent to the halo area. To our knowledge, this pattern of development has not been reported for the tapetum of any other species.

The unusual appearance of the tapetal plastids occurs just prior to the onset of sporopollenin deposit. We concluded that the plastids were synthesizing sporopollenin precursors. Until recently, sporopollenin was considered a carotenoid polymer (Brooks and Shaw 1968). New evidence has demonstrated that it is largely derived from a variety of saturated fatty acids (Guilford et al. 1988). The fact that chloroplasts synthesize saturated fatty acids suggested to us that these plastids might be doing likewise. The close proximity of rough ER to these plastids suggested a route through which the precursors could be moved through the tapetum to the perimeter of the locule. We did not observe vesicles fusing with the plasma membrane, however. The transfer may involve extrusion of these precursors directly through the lipid bilayer. Even though 58.8% of the sporopollenin is deposited into the exine after these plastids begin to senesce, we feel that the precursor synthesis could be complete prior to the onset of senescence, followed later by a polymerization phase.

The tapeta showed two distinct developmental patterns. In the majority of microsporangia (seen in anther cross sections) the tapetal cells had rectangular contours, but in others they became enlarged, protruded into the locule, and crowded the developing microspores. Correlated with hypertrophied tapeta was the more frequent occurrence of young microspores having nonspherical, amoeboid shapes, and in the process of degeneration. These tapeta showed a delay in the normal phase of degeneration. The enlarged tapetal cells were evident in 35% ($n=17$) of untreated microsporangia in the young free microspore stage, in 30% ($n=23$) of microsporangia in the vacuolate microspore stage, but were absent from the vacuolate pollen grain and near-mature pollen stage. Brooks et al. (1966) showed that enlarged tapeta in cytoplasmic male-sterile sorghum were correlated with pollen abortion. We concluded that the tapeta with rectangular contours represented the normal pattern of development and that the locules with hypertrophied tapeta were not sampled in the pollen grain stages because they had aborted.

Sources of sporopollenin precursors

The question of whether the precursors for the exine wall and Ubisch bodies are synthesized in the

tapetum or microspore, or both, has long been a topic of debate (see de Vries and Ie 1970). Autoradiographic data from *Lilium* anthers (Taylor 1959) suggest that the source of one type of wall precursor is the tapetum: sulfur-35 is incorporated into the exine wall and Ubisch bodies; tapetal cells also bind the label; however, the microspore cytoplasm binds relatively little. One might predict an increased synthesis of messenger RNA and protein for the wall polymerizing enzymes. Such an increase in both messenger RNA and protein was reported for tapetal cells just prior to deposition of the exine, while little of either was shown for microspores (Taylor 1959). Histochemical analysis of *Triticum durum* (Rudramuniyappa and Panchaksharappa 1980) revealed a pattern similar to that of *Lilium:* meiocytes and young microspores showed low rates of protein and RNA synthesis, while tapetal cells were rich in proteins and RNA before meiosis and continued to stain densely for proteins throughout development.

Anther development in plants treated with RH0007

Microspores of treated plants developed normally through meiosis and then aborted during or shortly after vacuolation. The exine wall of these cell contained less sporopollenin than that of the untreated controls. Reduced dosages of treatment resulted in proportionately thicker walls. Two possibilities were considered for the effects of RH0007 on development – that it interfered with the synthesis of sporopollenin precursors, and/or that it interfered with the polymerization of the precursors into the exine wall. Preliminary spectrophotometric analysis of anthers extracted for carotenoids showed slightly greater quantities of the pigments in treated anthers than in controls (unpublished observations). We concluded that the effect of the chemical hybridizing agent is on the polymerization of the precursors into the exine wall. Microspores became plasmolyzed and aborted at the stage of vacuolation, a time when rapid water uptake is necessary for vacuolation to occur. Large quantities of unpolymerized carotenoids in the locule could have caused the plasmolysis and subsequent death of these microspores.

Tapetal cells of treated plants showed normal development through the meiosis stage. Pro-Ubisch bodies were extruded onto the plasma membrane surface, but sporopollenin deposit was uneven and sparce, as was seen for the exine. Tapetal plastids acquired a halo, and the ER was associated with these plastids as in the untreated controls.

The pattern of dense globules observed in the halo of some tapetal plastids presented an enigma. It was seen less frequently in treated plants (31%) than in controls (41%). We ruled it out as a sign of anther degeneration, since it was restricted to tapetal cells, and these cells did not appear to be degenerating. We hazard the guess that the deposits might be a precipitation of sporopollenin precursors since they were also found on the tapetal surface inside the locule. The difficult question to explain is what the deposit might be doing next to mitochondria. The deposit was found too frequently to say that it was an anomaly, and it was found in both types of tapeta, expanded and rectangular. We are unsure of the significance of this phenomenon but felt it important to report.

Dense globular deposits were also seen in some microspore plastids of RH0007-treated plants. A portion of the microspore plastids in both control and treated plants appeared to undergo degeneration. Since the globules were restricted to treated plants only, where the whole cell was degenerating, we reasoned that it was less likely that these globules could be precipitation of sporopollenin. It appears to us that precursors for the exine and orbicular wall are synthesized exclusively in the tapetal plastids.

References

Bennett MD, Rao MK, Smith JB, Bayliss MW (1973) Cell development in the anther, the ovule, and the young seed of *Triticum aestivum* L. var. 'Chinese Spring'. Philos Trans R Soc London Ser B 266:39–81

Brooks JS, Shaw G (1968) The post-tetrad ontogeny of the pollen wall and the chemical structure of the sporopollenin of *Lilium henryi*. Grana Palynol 8:227–234

Brooks MH, Brooks JS, Chien L (1966) The anther tapetum in cytoplasmic-genetic male-sterile sorghum. Am J Bot 53:902–908

Christensen JE, Horner HT, Jr (1974) Pollen pore development and its spatial orientation during microsporogenesis in the grass *Sorghum bicolor*. Am J Bot 61:604–623

Christensen JE, Horner HT, Jr, Lersten NR (1972) Pollen wall and tapetal orbicular wall development in *Sorghum bicolor* (Gramineae). Am J Bot 59:43–58

deVries AP, Ie TS (1970) Electron-microscopy on anther tissue and pollen of male-sterile and fertile wheat (*Triticum aestivum* L.). Euphytica 19:103–120

Dickinson JG, Helop-Harrison J (1970) The ribosome cycle, nucleoli, and cytoplasmic nucleoids in the meiocytes of *Lilium*. Protoplasma 69:187–200

Echlin P, Godwin H (1969) The ultrastructure and ontogeny of pollen in *Helleborus foetidus* L. III. The formation of the pollen grain wall. J Cell Sci 5:459–477

El-Ghazaly G, Jensen WA (1986) Studies of the development of wheat (*Triticum aestivum*) pollen. I. Formation of the pollen wall and Ubisch bodies. Grana 25:1–29

Guilford WJ, Schneider DM, Labovitz J, Opella SJ (1988) High-resolution solid state C-NMR spectroscopy of sporo-

pollenins from different plant taxa. Plant Physiol 89:134–136
Heslop-Harrison J (1968) Some fine structural features of intine growth in the young microspore of *Lilium henryi*. Port Acta Biol Ser A 10:235–244
Heslop-Harrison J (1971) The cytoplasm and its organelles during meiosis. In: Heslop-Harrison J (ed) Pollen: development and physiology. Appleton-Century-Crofts, New York, pp 16–31
Hu S, Wang M, Hsu L (1977) Electron-microscopic observations on the microsporogenesis in male sterile and its maintainer lines of wheat. Sci Sin 20:625–630
Hu S, Zhu C, Xu L, Li X, Shen J (1979) Ultrastructure of male gametophyte in wheat. I. The formation of generative and vegetative cells. Acta Bot Sin 21:208–214
Lee SJ, Warmke HE (1979) Organelle size and number in fertile and T-cytoplasmic male-sterile corn. Am J Bot 66:141–148
Lee SJ, Earle ED, Gracen VE (1980) The cytology of pollen abortion in S cytoplasmic male-sterile corn anthers. Am J Bot 67:237–245
Lee SJ, Gracen VE, Earle ED (1979) The cytology of pollen abortion in C-cytoplasmic male-sterile corn anthers. Am J Bot 66:656–667
Maheshwari P (1950) Introduction to embryology of angiosperms. McGraw-Hill, New York
Overman MA, Warmke HE (1972) Cytoplasmic male sterility in sorghum. II. Tapetal behavior in fertile and sterile anthers. J Hered 65:227–234
Peterson RF (1965) Wheat: botany, cultivation and utilization, Interscience, New York, pp 22–23
Reynolds ES (1963) The use of lead citrate at high pH as an electron opaque stain in electron microscopy. J Cell Biol 17:208–212
Rowley JR (1962a) Nonhomogeneous sporopollenin in microspores of *Poa annua* L.. Grana Palynol 3:3–20
Rowley JR (1962b) Stranded arrangement of sporopollenin in the exine of microspores of *Poa annua*. Science 137:526–528
Rowley JR (1963) Ubisch body development in *Poa annua*. Grana Palynol 4:25–36
Rowley JR (1964) Formation of the pore in pollen in *Poa annua*. In: Linskens HF (ed) Pollen physiology and fertilization. North Holland, Amsterdam, pp 59–69
Rudramuniyappa CK, Panchaksharappa MG (1980) Pollen development in *Triticum durum* Desf.: a histochemical study. J S Afr Bot 46:33–43
Schulz P, Jensen WA (1981) Pre-fertilization ovule development in *Capsella:* ultrastructure and ultracytochemical localization of acid phosphatase in the meiocyte. Protoplasma 107:27–45
Skvarla JJ, Larson DA (1966) Fine structural studies of *Zea mays* pollen. I. Cell membranes and exine ontogney. Am J Bot 53:1112–1125
Spurr AR (1969) A low viscosity expoxy resin embedding medium for electron microscopy. J Ultrastruct Res 26:31–43
Taylor JH (1959) Autoradiographic studies of nucleic acids and proteins during meiosis in *Lilium longiflorum*. Am J Bot 46:477–484
Warmke HE, Overman MA (1972) Cytoplasmic male sterility in *Sorghum*. I. Callose behavior in fertile and sterile anthers. J Hered 63:103–108
Warmke HE, Lee SJ (1977) Mitochondrial degeneration in Texas cytoplasmic male-sterile corn anthers. J Hered 68:213–222
Warmke HE, Lee SJ (1978) Pollen abortion in T cytoplasmic male-sterile corn (*Zea mays*): a suggested mechanism. Science 200:561–563
Young BA, Schulz-Schaeffer J, Carroll TW (1979) Anther and pollen development in male-sterile intermediate wheatgrass plants derived from wheat × wheatgrass hybrids. Can J Bot 57:602–618
Zhu C, Hu S, Xu L, Li W, Shen J (1979) The ultrastructure of sperm cells in wheat pollen grains (in chinese). Sci Sin 22:1017–1021